Journal of Materials Chemistry B

PAPER

View Article Online
View Journal | View Issue

Cite this: J. Mater. Chem. B, 2019, 7, 6822

A fluorescent probe for simultaneously sensing NTR and hNQO1 and distinguishing cancer cells†

Fanpeng Kong,‡ Ying Li,‡ Chao Yang, Xiao Li, Junlin Wu, Xiaojun Liu, Xiaonan Gao, Kehua Xu* and Bo Tang *

Received 29th July 2019,
Accepted 29th September 2019

DOI: 10.1039/c9tb01581g

rsc.li/materials-b

Identifying cancer at the cellular level during an early stage offers the hope of greatly improved outcomes for cancer patients. As potential cancer biomarkers, nitroreductase (NTR) and human quinine oxidoreductase 1 (hNQO1) are overexpressed in many type of cancer cells. Simultaneous detection of these two biomarkers would benefit diagnostic precision in related cancers without yielding false positive results. Herein, based on a dye generated *in situ* strategy, a dual-enzyme-responsive probe, CNN, was rationally designed and synthesized by installing *p*-nitrobenzene and trimethyl-locked quinone propionic acid groups, which are specific for NTR and hNQO1, respectively, into a single fluorophore. This probe is only activated in the presence of both NTR and hNQO1 and produces a large fluorescence response, enabling the detection of both endogenous NTR and hNQO1 activity in living cells. The imaging results indicate that the CNN probe differentiates cancer cells (HeLa, MDA-MB-231 and HepG2 cells) from normal liver HL-7702 cells owing to the existence of relatively high endogenous levels of both biomarkers in these cancer cells.

Introduction

Cancer is a substantial public health problem and the second leading cause of death worldwide.[1,2] Most cancer deaths are caused by the spread of cancer cells from primary tumor cells to distal organs (metastasis). Therefore, the survival of cancer patients is strongly associated with the tumor stage at the time of diagnosis. Clinical identification of tumor biomarkers holds great potential for rapid prediction of cancer diagnosis and offers the hope of greatly improved outcomes for cancer patients.[3] Among numerous tumor markers, overexpressed proteases are promising candidate enzymes to leverage both diagnostically and therapeutically as they play critical roles in cancer progression.[4]

Redox enzymes regulate redox homeostasis in living systems, and their abnormal regulation is implicated in a variety of cancers. For example, the activity of methionine sulfoxide reductases is known to be a crucial biomarker for human breast cancers.[5] Tyrosine oxidase is implicated in melanoma cancer. Cyclooxygenase 2 (COX-2) is frequently overexpressed in non-small cell lung cancer and is associated with aggressive tumors and poor patient outcomes.[6] Overexpressed thioredoxin reductase (TrxR) is expressed at high levels in a wide variety of human tumors including lung, pancreas, colon, gastric and breast cancer.[7] Cytochrome P450 1A (CYP 1A) is highly expressed in a wide range of tumor types and may greatly contribute to the development and progression of cancer.[8] Detection of tumor-related overexpression of redox enzymes provides new tools for discriminating a wide range of cancer cells both *in vitro* and *in vivo*. Fluorescence-guided diagnostics is one of the most powerful real-time techniques for *in situ* tumor detection[9] due to its high sensitivity, low cost, portability, and real-time capabilities.[10–12] Multiple fluorescent probes for detecting tumor specific redox enzymes and other protease overexpression in complex biological specimens have been reported.[13–25]

Nitroreductase (NTR) is an indicator of highly aggressive disease in various hypoxic tumor cells,[26,27] and overexpression of NTR during hypoxia plays an important role in malignant tumor progression and angiogenesis. Human NAD(P)H: quinone oxi-doreductase isozyme I (hNQO1) is markedly upregulated in many types of cancer cells and solid tumors.[28] Importantly, hNQO1 overexpression has been directly linked to both tumor genesis and poor patient survival.[29] Therefore, early and accurate NTR and hNQO1 detection is likely important for cancer diagnosis. Many fluorescence probes have been synthesized for the detection and imaging of NTR[30–36] and hNQO1[37–42] in cancer cells. However, detecting a single tumor related overexpressed protease may yield false positive results, restricting identification of cancer.

College of Chemistry, Chemical Engineering and Materials Science, Institute of Biomedical Sciences, Collaborative Innovation Center of Functionalized Probes for Chemical Imaging in Universities of Shandong, Key Laboratory of Molecular and Nano Probes, Ministry of Education, Shandong normal University, Jinan 250014, P. R. China. E-mail: tangb@sdnu.edu.cn, xukehua@sdnu.edu.cn

† Electronic supplementary information (ESI) available: Experimental procedures, synthesis of the probe, ^{1}H NMR, ^{13}C NMR and HRMS data and MTT assay. See DOI: 10.1039/c9tb01581g

‡ These authors contributed equally to this work.

Simultaneous detection of multiple tumor markers brings new opportunities for improving the accuracy of early cancer detection compared to the single-marker assay.[43–45] Recently, various platforms using nanomaterials for the detection of multiple targets have been developed,[46–50] but relatively few molecular probes have been developed that detect multiple tumor markers simultaneously.[51] Herein, we report a dual site fluorescence probe, **CNN**, to which a 4-nitrobenzene moiety and trimethyl-locked quinone propionic acid (Q3PA) were introduced as reaction units, as well as a fluorescence quencher. In the presence of NTR and hNQO1, **CNN** exhibited a dramatic off–on fluorescence response, while other potential interfering species, including inorganic salts, amino acids, thiols, reactive oxygen species (ROS) and glucose, elicited no significant fluorescence. Cellular imaging experiments clearly indicated that **CNN** differentiates cancer cells from normal cells owing to the existence of relatively high endogenous levels of both biomarkers.

Results and discussion

The **CNN** probe design is based on *in situ* formation of blue emitting 7-hydroxy (2-imino)coumarin[52–54] generated from a caged bifunctional precursor through effective domino reactions triggered by NTR and hNQO1 (Scheme 1a). The *p*-nitrobenzene group and trimethyl-locked quinone propionic acid (Q3PA) were utilized, which are specific for NTR and hNQO1, respectively. In the absence of NTR and hNQO1, the fluorescence of the **CNN** probe was quenched by the electron-withdrawing effect of the 4-nitrobenzene moiety and Q3PA due to PET inhibition. In the presence of hNQO1 only, the Q3PA group of the **CNN** probe was removed, releasing compound **A**, which still showed no fluorescence due to linking the 4-nitrobenzene quencher group. In contrast, the *p*-nitrobenzene group was reduced to the aminobenzene group by NTR in the presence of NADH, followed by a 1,6-rearrangement elimination reaction, resulting in the formation of a coumarin derivative (compound **B**). However, the fluorescence of compound **B** was very low because the Q3PA group is an effective photo-induced electron transfer (PeT) quencher of fluorescence due to its electron deficient nature. Treatment of **CNN** with NTR and hNQO1 together resulted in strong fluorescence enhancement due to formation of 7-hydroxy-(2-imino)coumarin (quantum yield, Φ = 0.16) (Fig. S1, ESI†). The sensing mechanism of **CNN** toward NTR and hNQO1 was validated by using HRMS (Fig. S2, ESI†). The synthesis route for the **CNN** probe is shown in Scheme 1. The structures of all intermediates and the final product were confirmed by nuclear magnetic resonance (NMR) and high resolution mass spectrometry (HRMS) (see the ESI†).

The fluorescence responses of the **CNN** probe to different concentrations of NTR and hNQO1 were investigated. As shown in Fig. 1a, **CNN** was initially non-fluorescent, and with the addition of NADH (50 μM) and hNQO1 (0.4 μg mL^{-1}) almost no fluorescence increase was observed. However, subsequent additions of NTR resulted in evident increases in fluorescence intensity. Furthermore, a good linear relationship exists between the fluorescence intensity at 454 nm and concentrations of NTR in the 0–2.0 μg mL^{-1} range (Fig. 1b), with R^2 = 0.992. The detection limit (k = 3) of the probe for NTR was determined as 10 ng mL^{-1}. Emission spectra of **CNN** were also recorded in PBS in the presence of NADH (50 μM) and NTR (2 μg mL^{-1}). As shown in Fig. 1c, a slight increase in fluorescence was observed, and subsequent additions of hNQO1 resulted in a much larger increase in fluorescence intensity. A linear functional relationship (R^2 = 0.993) was obtained between the fluorescence

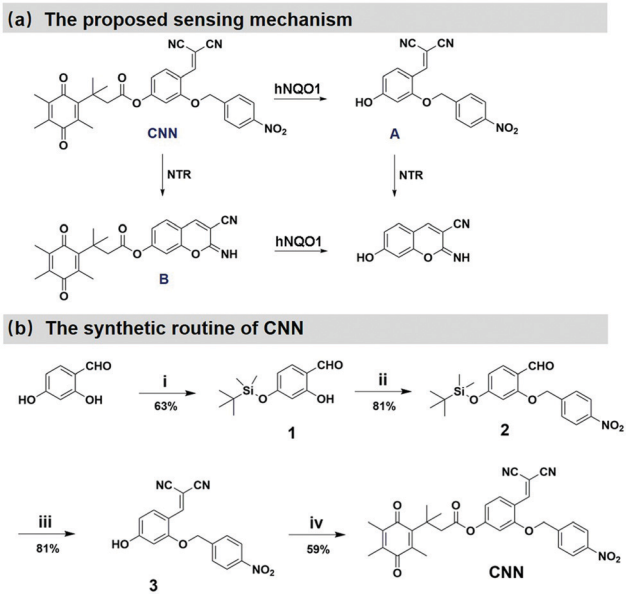

Scheme 1 (a) Potential reaction mechanism of **CNN** for NTR and hNQO1 detection and (b) synthesis of the probe CNN.

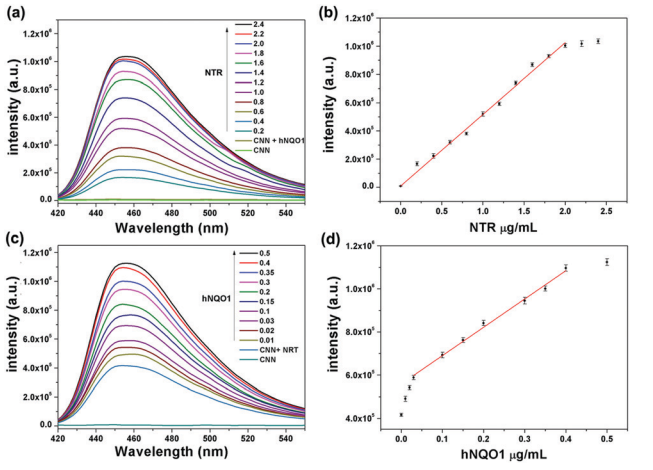

Fig. 1 (a) Fluorescence spectra of **CNN** (5 μM) after adding different concentrations of NTR (0–2.4 μg mL^{-1}) in the presence of hNQO1 (0.4 μg mL^{-1}) and NADH (50 μM). (b) The linear relationship between the fluorescence intensity and the concentration of NTR. (c) Fluorescence spectra of **CNN** (5 μM) after adding different concentrations of hNQO1 (0–0.5 μg mL^{-1}) in the presence of NTR (2.0 μg mL^{-1}) and NADH (50 μM). (d) The linear relationship between the fluorescence intensity and the concentration of hNQO1.

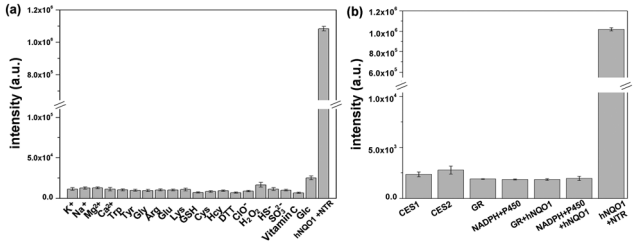

Fig. 2 (a) Fluorescence responses of **CNN** (5 μM) upon treatment with various biologically-relevant species. (b) Fluorescence responses of **CNN** (5 μM) against different enzymes.

intensity at 454 nm and hNQO1 concentrations (0–0.4 μg mL^{-1}) with a detection limit as low as 2 ng mL^{-1} based on the $3s/k$ principle. These results indicate that the **CNN** probe requires both NTR and hNQO1 for a fluorescence response.

The specificity of the **CNN** probe was evaluated for NTR and hNQO1 over other potential interfering species, including inorganic salts, amino acids, thiols, ROS, glucose and two different kinds of biologically-relevant species (Fig. S3, ESI†). In addition, the selectivity of the probe to carboxylesterase **1** (CES1), carboxylesterase **2** (CES2), glutathione reductase (GR) and P450 cytochrome reductase in the presence of hNQO1 was also examined. As illustrated in Fig. 2, addition of other species exhibited a negligible fluorescence response, with only combined NTR and hNQO1 inducing remarkable fluorescence enhancement. All data revealed that **CNN** exerts excellent specificity under physiological conditions. Furthermore, to evaluate the compatibility of CNN with biological systems, the cytotoxicity of the probe was evaluated in HeLa and HepG2 cells using a standard MTT assay (Fig. S4, ESI†). The cell viability remained over 80% after incubation with even high concentrations of the probe (20 μM), indicating good biocompatibility of the probe with cells. The photostability of the fluorescent product **CNN** was also evaluated. After illumination at 405 nm by a 150 W xenon lamp for 10 min, the fluorescence intensity of **CNN** buffer solution remained at 90% (Fig. S5, ESI†), indicating good photostability of the dye under the detection conditions.

Encouraged by the results described above, we next examined the potential use of **CNN** for visualizing NTR and hNQO1 in living cells to investigate whether **CNN** could be employed to distinguish different types of cancer cells. Given the elevated levels of both NTR and hNQO1 in some cancer cells, three types of solid tumor cells, HeLa, MDA-MB-231 and HepG2 cells, and normal liver HL-7702 cells were selected for evaluation. To simulate the solid tumor hypoxic microenvironment, HeLa, MDA-MB-231 and HepG2 cells were incubated under hypoxic conditions (1% p_{O_2}) for 4 h compared to the control group (HL-7702 cells in normoxic conditions 20% p_{O_2}). Excitingly, all three cancer cell lines incubated with the CNN probe showed strong fluorescence in the green channel, whereas almost no intracellular fluorescence was observed in the normal cell line (Fig. 3a). The mean fluorescence intensity in the cancer cell lines was consistently more than 3 times higher than that in the normal cell line (Fig. 3b), indicating that NTR and hNQO1 have the potential to be ubiquitous tumor markers using CNN as a highly effective probe to differentiate cancer cells from normal cells.

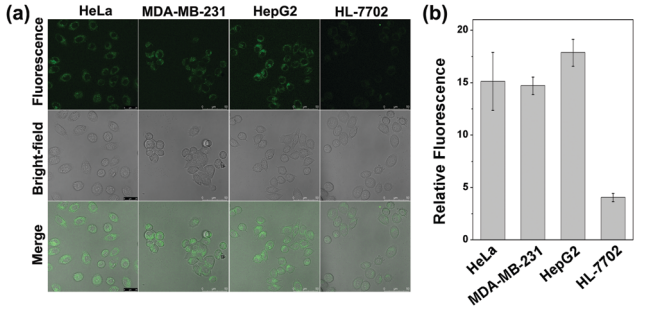

Fig. 3 (a) Confocal fluorescence microscope images for endogenous NTR and hNQO1 detection in different cell lines using CNN (10 μM). (b) Relative fluorescence intensity of the images from (a).

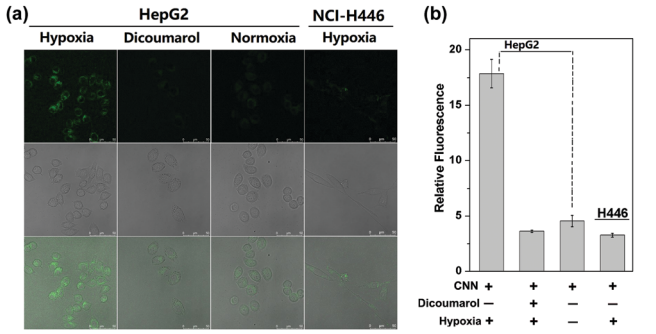

Fig. 4 (a) Confocal fluorescence microscope images for endogenous NTR and hNQO1 detection in HepG2 cells and NCI-H446 cells using **CNN** (10 μM) under different conditions. (b) Relative fluorescence intensity of the images from (a).

To further confirm activation of CNN in cancer cells in response to both NTR and hNQO1, we added dicoumarol, an NTR and hNQO1 inhibitor, or incubated HepG2 cells with the CNN probe in aerobic conditions, which causes low expression of NTR. As shown in Fig. 4a, HepG2 cells incubated with the CNN probe under hypoxic conditions yielded bright fluorescence. In contrast, in the inhibitor-treated group and the group incubated in aerobic conditions, HepG2 cells showed very weak fluorescence with an observed mean fluorescence intensity only a third of that in the group without inhibitors (Fig. 4b). In addition, NCI-H446 cells (a small-cell lung carcinoma known to be devoid of hNQO1 activity)[55] were also used for evaluating the role of hNQO1 in the probe activation. As shown in Fig. 4, even in hypoxic conditions, the probe cannot be activated in NCI-H446 cells due to the lack of hNQO1. These results clearly demonstrated the dual NTR and hNQO1 requirement for CNN function.

Experimental

General chemicals and instruments

2,4-Dihydroxybenzaldehyde, imidazole, *tert*-butyldimethylsilyl chloride, dichloromethane, absolute ethanol, silver oxide, tetrahydrofuran, 1-ethyl-(3-dimethylaminopropyl)carbonyldiimide hydrochloride and 4-nitrobenzyl bromide were purchased from Energy Chemical. Malononitrile was purchased from Sun Chemical Technology Co., Ltd (Shanghai, China). Anhydrous magnesium sulfate,

anhydrous ether, piperidine, and tetrahydrofuran were purchased from Sinopharm Chemical Reagent Co., Ltd (Shanghai, China). β-NADH was purchased from Aladdin Reagent Co., Ltd (Shanghai, China). β-NADPH was purchased from Aladdin Reagent Co., Ltd (Shanghai, China). NTR from *Escherichia coli* was purchased from Sigma Chemical Company. hNQO1 from *Escherichia coli* was purchased from ProSpec-Tany TechnoGene Ltd. Recombinant Human CES1 is produced by our mammalian expression system and purchased from Novoprotein Scientific Inc. Human CES2 is expressed by human HEK293 cells and purchased from Sino Biological. Glutathione reductase was purchased from Solarbio. NADPH-P450 cytochrome reductase was purchased from ProSpec-Tany TechnoGene Ltd. Dicoumarol was purchased from Medchem Express (MCE). All chemicals and solvents used for synthesis were purchased from commercial suppliers and applied directly in the experiments without further purification. ^{1}H NMR and ^{13}C NMR spectra were recorded on a Bruker Advance 400 MHz spectrometer at room temperature. UV-vis absorption spectra were measured on a UV-visible spectrophotometer (UV-1700 Pharmaspec, Shimadzu, Japan). All pH measurements were performed with a pH-3c digital pH-meter (Shanghai LeiCi Device Works, Shanghai, China) with a combined glass–calomel electrode. Mass spectra were obtained using a Bruker maXis ultrahigh resolution-TOF MS system. Fluorescence spectra were measured on an FLS-980 Edinburgh fluorescence spectrometer. Cellular bioimaging was carried out on a confocal microscope (Leica TCS SP8). Absorbance was measured with a microplate reader (Synergy 2, Biotek, USA) in the MTT assay.

Synthesis of probe CNN

Synthesis of compound 1. 2,4-Dihydroxybenzaldehyde (2 g, 14.5 mmol) and imidazole (1.15 g, 16.9 mmol) were dissolved in dichloromethane, and stirred at room temperature for 5 min under an argon atmosphere, followed by addition of *tert*-butyldimethylsilyl chloride (2.2 g, 14.5 mmol). The mixture was then stirred at room temperature for 4 hours, and the progress of the reaction was monitored by TLC. After the reaction was complete, the residue was washed with deionized water and brine, and the organic phases were combined. The organic phase was dried with anhydrous magnesium sulfate, and the solvent was removed under reduced pressure. The residue was purified using silica gel column chromatography with PE/EA (15/1), yielding a colorless oily liquid (2.3 g, 63%). The ^{1}H NMR properties and findings are as follows: (400 MHz, $CDCl_3$) δ 11.35 (s, 1H), 9.73 (s, 1H), 7.41 (d, J = 8.5 Hz, 1H), 6.54–6.34 (m, 2H), 0.99 (s, 9H), 0.28–0.25 (m, 6H). ^{13}C NMR (101 MHz, $CDCl_3$) δ 194.5, 164.1, 163.8, 135.4, 115.8, 113.0, 107.6, 77.4, 77.0, 76.7, 25.7–25.4 (3C), −4.1 to 4.4 (3C). HRMS, calculated for $C_{13}H_{20}O_3Si$ $[M - H]^-$ m/z 251.1097, found 251.1082.

Synthesis of compound 2. Compound **1** (2 g, 8 mmol) and silver oxide (7.4 g, 32 mmol) were added to anhydrous ether and stirred for 5 min, followed by addition of 4-nitrobenzyl bromide (8.6 g, 40 mmol). The reaction progress was monitored by TLC. After the reaction was over, excess silver oxide was filtered off, the solvent was removed under reduced pressure, and the residue was purified using a silica gel column with PE/EA(10/1), which yielded a white solid (2.5 g, 81%). The ^{1}H NMR properties and findings are as follows: (400 MHz, $CDCl_3$) δ 10.18 (s, 1H), 8.07 (d, J = 8.6 Hz, 2H), 7.58 (d, J = 8.5 Hz, 1H), 7.43 (d, J = 8.6 Hz, 2H), 6.32 (d, J = 8.5 Hz, 1H), 6.19 (d, J = 1.8 Hz, 1H), 5.04 (s, 2H), 0.75 (s, 9H), −0.00 (s, 6H). ^{13}C NMR (101 MHz, $CDCl_3$) δ 187.8, 162.9, 161.8, 147.8, 143.3, 131.0, 127.5, 124.0, 119.6, 113.4, 104.6, 77.3, 77.0, 76.7, 69.0, 25.5, −4.3. HRMS, calculated for $C_{20}H_{25}NO_5Si$ $[M + H]^+$ m/z 388.1574, found 388.1567.

Synthesis of compound 3. Compound **2** (466 mg, 1.2 mmol) and malononitrile (85 mg, 1.26 mmol) were dissolved in absolute ethanol followed by addition of a catalytic amount of piperidine and stirred at room temperature for 1 hour. The reaction progress was monitored by TLC. After the reaction was complete, the solvent was removed under reduced pressure. The residue was dissolved in tetrahydrofuran (15 mL), and tetrabutylammonium fluoride (1.4 mL) was subsequently added and stirred at room temperature for 5 min. The reaction was monitored by TLC. After the reaction was complete, the solvent was removed under reduced pressure. Dichloromethane was added, washed with deionized water, and then washed with 1.0 M HCl and brine. The solvent was dried over anhydrous sodium sulfate and removed under reduced pressure. Recrystallization from methanol yielded an orange solid (175 mg, 45%). The ^{1}H NMR properties and findings are as follows: (400 MHz, DMSO-d_6) δ 11.21 (s, 1H), 8.46–8.14 (m, 3H), 8.06 (d, J = 8.7 Hz, 1H), 7.78 (d, J = 8.2 Hz, 2H), 6.78–6.42 (m, 2H), 5.40 (s, 2H). ^{13}C NMR (101 MHz, DMSO-d_6) δ 166.6, 160.6, 153.9, 147.6, 144.2, 131.0, 128.9, 124.1, 116.0, 114.9, 112.6, 110.3, 101.0, 74.8, 69.3, 40.6, 40.4, 40.2, 40.0, 39.7, 39.5, 39.3. HRMS calculated for $C_{17}H_{11}N_3O_4$ $[M - H]^-$ m/z 320.0665, found 320.0701.

Synthesis of the CNN probe. Compound **3** (175 mg, 0.54 mmol), 3-methyl-3-(2,4,5-trimethyl-3,6-dioxocyclohexyl-1,4-dienyl)butyric acid (150 mg, 0.6 mmol) and 1-ethyl-(3-dimethylaminopropyl)carbonyldiimide hydrochloride (157 mg, 0.8 mmol) were dissolved in dichloromethane and stirred at room temperature overnight. After the reaction was complete, the residue was washed with deionized water, and the organic phases were combined. The organic phase was dried with anhydrous sodium sulfate, and the solvent was removed under reduced pressure. The residue was purified using silica gel column chromatography with PE/EA (10/1) to yield a light yellow solid (178 mg, 59%). The ^{1}H NMR properties and findings are as follows: (400 MHz, $CDCl_3$) δ 8.31 (d, J = 8.6 Hz, 2H), 8.25 (d, J = 8.8 Hz, 1H), 8.19 (s, 1H), 7.59 (t, J = 10.7 Hz, 2H), 6.82 (dd, J = 8.7, 1.9 Hz, 1H), 6.73 (d, J = 1.9 Hz, 1H), 5.22 (d, J = 11.9 Hz, 2H), 3.27 (s, 2H), 2.19 (s, 3H), 1.94 (d, J = 9.6 Hz, 6H), 1.52 (s, 6H). ^{13}C NMR (101 MHz, $CDCl_3$) δ 190.6, 187.3, 170.3, 158.4, 156.6, 152.6, 150.9, 148.20, 142.5, 141.7, 139.9, 139.0, 130.2, 128.1, 124.2, 118.0, 115.5, 114.0, 112.7, 106.4, 82.0, 77.3, 77.0, 76.7, 69.9, 58.4, 47.6, 38.4, 29.1, 18.4, 14.5, 12.6, 12.2. HR-MS, calculated for $C_{31}H_{27}N_3O_7$ $[M + Na]^+$ m/z 576.1741, found 576.1731.

Conclusions

In summary, a novel dual-site fluorescent probe, **CNN**, for the simultaneous detection of two potential cancer biomarkers,

NTR and hNQO1, has been developed for the first time. The **CNN** probe exhibits high sensitivity, excellent selectivity and good biocompatibility. In the presence of both NTR and hNQO1, the fluorescence of the **CNN** probe was significantly enhanced *via* an *in situ* generated coumarin dye, enabling the **CNN** probe to distinguish between cancer cells and normal cells due to the notably high endogenous levels of NTR and hNQO1 in these cancer cells. We thus anticipate that the **CNN** probe has potential application for identifying cancer at the cellular level during early stages, and can provide a simple and convenient new method for the early diagnosis of cancer. However, the relatively short emission wavelength is a potential limitation of this probe. We are currently working to develop near-infrared dual-responsive probes for *in vivo* applications.

Conflicts of interest

There are no conflicts to declare.

Acknowledgements

This work was supported by the National Natural Science Foundation of China (21874085, 21535004, 91753111 and 21775091) and the Key Research and Development Program of Shandong Province (2018YFJH0502).

Notes and references

1 R. L. Siegel, K. D. Miller and A. Jemal, *Ca-Cancer J. Clin.*, 2018, **68**, 7–30.
2 F. Bray, A. Jemal, N. Grey, J. Ferlay and D. Forman, *Lancet Oncol.*, 2012, **13**, 790–801.
3 G. Blum, G. Von Degenfeld, M. J. Merchant, H. M. Blau and M. Bogyo, *Nat. Chem. Biol.*, 2007, **3**, 668–677.
4 C. A. K. Borrebaeck, *Nat. Rev. Cancer*, 2017, **17**, 199–204.
5 A. De Luca, F. Sanna, M. Sallese, C. Ruggiero, M. Grossi, P. Sacchetta, C. Rossi, V. De Laurenzi, C. Di Ilio and B. Favaloro, *Proc. Natl. Acad. Sci. U. S. A.*, 2010, **107**, 18628–18633.
6 I. Csiki, K. Yanagisawa, N. Haruki, S. Nadaf, J. D. Morrow, D. H. Johnson and D. P. Carbone, *Cancer Res.*, 2006, **66**, 143–150.
7 G. Powis and D. L. Kirkpatrick, *Curr. Opin. Pharmacol.*, 2007, **7**, 392–397.
8 Q. Ma and A. Y. Lu, *Chem. Res. Toxicol.*, 2003, **16**, 249–260.
9 D. Asanuma, M. Sakabe, M. Kamiya, K. Yamamoto, J. Hiratake, M. Ogawa, N. Kosaka, P. L. Choyke, T. Nagano, H. Kobayashi and Y. Urano, *Nat. Commun.*, 2015, **6**, 6463.
10 J. V. Frangioni, *J. Clin. Oncol.*, 2008, **26**, 4012–4021.
11 J. Zhang, X. Chai, X. P. He, H. J. Kim, J. Yoon and H. Tian, *Chem. Soc. Rev.*, 2019, **48**, 683–722.
12 R. Weissleder and M. J. Pittet, *Nature*, 2008, **452**, 580–589.
13 H. Kobayashi, M. Ogawa, R. Alford, P. L. Choyke and Y. Urano, *Chem. Rev.*, 2010, **110**, 2620–2640.
14 Y. Urano, *Curr. Opin. Chem. Biol.*, 2012, **16**, 602–608.
15 A. A. Beharry, S. Lacoste, T. R. O'Connor and E. T. Kool, *J. Am. Chem. Soc.*, 2016, **138**, 3647–3650.
16 F. Wang, Y. Zhu, L. Zhou, L. Pan, Z. Cui, Q. Fei, S. Luo, D. Pan, Q. Huang, R. Wang, C. Zhao, H. Tian and C. Fan, *Angew. Chem., Int. Ed.*, 2015, **54**, 7349–7353.
17 X. Zhen, J. Zhang, J. Huang, C. Xie, Q. Miao and K. Pu, *Angew. Chem., Int. Ed.*, 2018, **57**, 7804–7808.
18 X. Chen, D. Lee, S. Yu, G. Kim, S. Lee, Y. Cho, H. Jeong, K. T. Nam and J. Yoon, *Biomaterials*, 2017, **122**, 130–140.
19 H. Zhang, J. Fan, J. Wang, B. Dou, F. Zhou, J. Cao, J. Qu, Z. Cao, W. Zhao and X. Peng, *J. Am. Chem. Soc.*, 2013, **135**, 17469–17475.
20 K. Gu, Y. Xu, H. Li, Z. Guo, S. Zhu, S. Zhu, P. Shi, T. D. James, H. Tian and W. H. Zhu, *J. Am. Chem. Soc.*, 2016, **138**, 5334–5340.
21 Y. Jiao, J. Yin, H. He, X. Peng, Q. Gao and C. Duan, *J. Am. Chem. Soc.*, 2018, **140**, 5882–5885.
22 Z. R. Dai, G. B. Ge, L. Feng, J. Ning, L. H. Hu, Q. Jin, D. D. Wang, X. Lv, T. Y. Dou, J. N. Cui and L. Yang, *J. Am. Chem. Soc.*, 2015, **137**, 14488–14495.
23 Z. R. Dai, L. Feng, Q. Jin, H. L. Cheng, Y. Li, J. Ning, Y. Yu, G. B. Ge, J. N. Cui and L. Yang, *Chem. Sci.*, 2017, **8**, 2795–2803.
24 J. Ning, W. Wang, G. Ge, P. Chu, F. Long, Y. Yang, Y. Peng, L. Feng, X. Ma and T. D. James, *Angew. Chem., Int. Ed.*, 2019, **58**, 9959–9963.
25 J. Ning, T. Liu, P. Dong, W. Wang, G. Ge, B. Wang, Z. Yu, L. Shi, X. Tian, X. Huo, L. Feng, C. Wang, C. Sun, J. Cui, T. D. James and X. Ma, *J. Am. Chem. Soc.*, 2019, **141**, 1126–1134.
26 M. C. Hung, G. B. Mills and D. Yu, *Nat. Med.*, 2009, **15**, 246–247.
27 W. R. Wilson and M. P. Hay, *Nat. Rev. Cancer*, 2011, **11**, 393–410.
28 D. Siegel, C. Yan and D. Ross, *Biochem. Pharmacol.*, 2012, **83**, 1033–1040.
29 X. Cui, L. Li, G. Yan, K. Meng, Z. Lin, Y. Nan, G. Jin and C. Li, *BMC Cancer*, 2015, **15**, 244.
30 H. W. Liu, X. B. Zhang, J. Zhang, Q. Q. Wang, X. X. Hu, P. Wang and W. Tan, *Anal. Chem.*, 2015, **87**, 8896–8903.
31 K. H. Gebremedhin, Y. Li, Q. Yao, M. Xiao, F. Gao, J. Fan, J. Du, S. Long and X. Peng, *J. Mater. Chem. B*, 2019, **7**, 408–414.
32 Y. Liu, L. Teng, L. Chen, H. Ma, H. W. Liu and X. B. Zhang, *Chem. Sci.*, 2018, **9**, 5347–5353.
33 A. Chevalier, Y. Zhang, O. M. Khdour, J. B. Kaye and S. M. Hecht, *J. Am. Chem. Soc.*, 2016, **138**, 12009–12012.
34 X. Tian, Z. Li, Y. Sun, P. Wang and H. Ma, *Anal. Chem.*, 2018, **90**, 13759–13766.
35 R. B. P. Elmes, *Chem. Commun.*, 2016, **52**, 8935–8956.
36 J. Zheng, Y. Shen, Z. Xu, Z. Yuan, Y. He, C. Wei, M. Er, J. Yin and H. Chen, *Biosens. Bioelectron.*, 2019, **119**, 141–148.
37 S. U. Hettiarachchi, B. Prasai and R. L. McCarley, *J. Am. Chem. Soc.*, 2014, **136**, 7575–7578.
38 Q. A. Best, A. E. Johnson, B. Prasai, A. Rouillere and R. L. McCarley, *ACS Chem. Biol.*, 2016, **11**, 231–240.
39 B. Prasai, W. C. Silvers and R. L. McCarley, *Anal. Chem.*, 2015, **87**, 6411–6418.

40 W. C. Silvers, B. Prasai, D. H. Burk, M. L. Brown and R. L. McCarley, *J. Am. Chem. Soc.*, 2013, **135**, 309–314.
41 S. Son, M. Won, O. Green, N. Hananya, A. Sharma, Y. Jeon, J. H. Kwak, J. L. Sessler, D. Shabat and J. S. Kim, *Angew. Chem., Int. Ed.*, 2019, **131**, 1739–1743.
42 N. Kwon, M. K. Cho, S. J. Park, D. Kim, S. J. Nam, L. Cui, H. M. Kim and J. Yoon, *Chem. Commun.*, 2017, **53**, 525–528.
43 J. D. Cohen, L. Li, Y. Wang, C. Thoburn, B. Afsari, L. Danilova, C. Douville, A. A. Javed, F. Wong, A. Mattox, R. H. Hruban, C. L. Wolfgang, M. G. Goggins, M. D. Molin, T. L. Wang, R. Roden, A. P. Klein, J. Ptak, L. Dobbyn, J. Schaefer, N. Silliman, M. Popoli, J. T. Vogelstein, J. D. Browne, R. E. Schoen, R. E. Brand, J. Tie, P. Gibbs, H. L. Wong, A. S. Mansfield, J. Jen, S. M. Hanash, M. Falconi, P. J. Allen, S. Zhou, C. Bettegowda, L. A. Diaz Jr., C. Tomasetti, K. W. Kinzler, B. Vogelstein, A. M. Lennon and N. Papadopoulos, *Science*, 2018, **359**, 926–930.
44 L. Liu, T. Li, S. Zhang, P. Song, B. Guo, Y. Zhao and H. C. Wu, *Angew. Chem., Int. Ed.*, 2018, **57**, 11882–11887.
45 J. D. Wulfkuhle, L. A. Liotta and E. F. Petricoin, *Nat. Rev. Cancer*, 2003, **3**, 267–275.
46 O. Braha, L. Q. Gu, L. Zhou, X. F. Lu, S. Cheley and H. Bay-Ley, *Nat. Biotechnol.*, 2000, **18**, 1005–1007.
47 X. Zhang, Y. Wang, B. L. Fricke and L. Q. Gu, *ACS Nano*, 2014, **8**, 3444–3450.
48 N. A. W. Bell and U. F. Keyser, *Nat. Nanotechnol.*, 2016, **11**, 645–651.
49 J. Y. Y. Sze, A. P. Ivanov, A. E. G. Cass and J. B. Edel, *Nat. Commun.*, 2017, **8**, 1552.
50 G. Celaya, J. Perales-Calvo, A. Muga, F. Moro and D. Rodriguez-Larrea, *ACS Nano*, 2017, **11**, 5815–5825.
51 C. Zhang, Q. Z. Zhang, K. Zhang, L. Y. Li, M. D. Pluth, L. Yi and Z. Xi, *Chem. Sci.*, 2019, **10**, 1945–1952.
52 D. Kim, S. Sambasivan, H. Nam, K. H. Kim, J. Y. Kim, T. Joo, K. H. Lee, K. T. Kim and K. H. Ahn, *Chem. Commun.*, 2012, **48**, 6833–6835.
53 D. Kim, S. Singha, T. Wang, E. Seo, J. H. Lee, S. J. Lee, K. H. Kim and K. H. Ahn, *Chem. Commun.*, 2012, **48**, 10243–10245.
54 S. Debieua and A. Romieu, *Org. Biomol. Chem.*, 2015, **13**, 10348–10361.
55 H. D. Beall, A. M. Murphy, D. Siegel, R. H. Hargreaves, J. Butler and D. Ross, *Mol. Pharmacol.*, 1995, **48**, 499–504.